

# Theoretical Study of the Hydrogen Bond Interaction Between Methylene Blue and Water and Possible Role on Energy Transfer for Photodynamics

ANDRÉA DIAS QUINTÃO,<sup>1</sup> KALINE COUTINHO,<sup>2</sup> SYLVIO CANUTO<sup>1</sup>

<sup>1</sup>Instituto de Física, Universidade de São Paulo, CP 66318, 05315-970 São Paulo, SP, Brazil

<sup>2</sup>Universidade de Mogi das Cruzes, CCET, CP 411, 08701-970, Mogi das Cruzes, SP, Brazil

Received 14 June 2001; accepted 5 September 2001

DOI 10.1002/qua.10059

**ABSTRACT:** Density-functional theory calculations using B3LYP/6-31+G(d) are performed on the hydrogen bond interaction between methylene blue (MB<sup>+</sup>) and water to analyze the structure, binding energy and change in spectroscopic properties. The vibrational frequency observed in the region of 1200 cm<sup>-1</sup> is found to present the larger shift (+10 cm<sup>-1</sup>), and corresponds to the asymmetric in-plane twist mode of C—C bond of the central ring. The binding energy between MB<sup>+</sup> and water is calculated for three different isomers giving values varying between 3.1 and 5.1 kcal/mol, after correcting for basis-set superposition error. The binding energy is also calculated using Hartree-Fock and other density-functionals, such as B3P86/6-31+G(d) and B3PW91/6-31+G(d). In the most stable isomer considered, the water plays the role of the proton acceptor and the oxygen atom makes multiple hydrogen bonds with MB<sup>+</sup>. The stability of this isomer is also influenced by other electrostatic interaction between MB<sup>+</sup> and water. The influence of the complexation on the characteristic visible absorption band of MB<sup>+</sup> is analyzed using INDO/CIS. Overall, the results indicate that several hydrogen bonds can be formed and some present multiple bonds. However, they all seem to be numerically unimportant for the photochemistry of MB<sup>+</sup> in water. © 2002 Wiley Periodicals, Inc. *Int J Quantum Chem* 90: 634–640, 2002

**Key words:** hydrogen bond; ab initio; methylene blue; photodynamics

Correspondence to: S. Canuto; e-mail: canuto@if.usp.br  
Contract grant sponsors: CNPq and FAPESP (Brasil).

## Introduction

**M**ethylene blue (MB) is a well-known molecule of considerable interest in chemistry and medicine [1]. It has been implicated in several medical aspects ranging from alcoholism to photodynamical therapy. In recent years several investigations have appeared related to coagulation factors [2], DNA damage [3] and binding [4], relaxing effects of venoms [5], photocatalysis [6], antiviral activities of HIV [7], cirrhosis [8], hepatopulmonary syndrome [9], reproduction and fertility [10], etc. MB has been implicated also as an emergency aid in underwater diving-related accidents [11]. There is an intense research related to the activity of MB in photodynamic therapy [12–16] and singlet-oxygen reactions [17–20]. MB is also a photodynamic antimicrobial agent [21] for the inactivation or destruction of pathogens contained in blood products. Obviously the theoretical study of MB activities for possible medical or chemical interest implies the necessity of understanding the activities of MB in solution. It is known that in water MB assumes its ionic form [22]  $\text{MB}^+$  and is a known ionic dye. Recent studies have shown that depending on the concentration,  $\text{MB}^+$  forms aggregates and that the aggregation is an important factor for understanding the spectroscopic factors of  $\text{MB}^+$  in solution [23, 24]. As water is the natural biological solvent it is also important to understand the interaction of  $\text{MB}^+$  with water. An important aspect of this interaction is the hydrogen bond [25, 26] between  $\text{MB}^+$  and water. The intermolecular forces involved in the dimer formation have been studied by Mukherjee and Ghosh [27]. From previous experimental investigations [22–24] it is expected that hydrogen bond interaction with water is important but should not play a decisive role on the spectroscopic properties. However, the precise extension of this has not been studied before. This is a point where quantum chemistry can clarify the matter. The field of quantum chemistry owes much to the pioneering work of Löwdin. A historical account is given in Ref. [28]. But he also showed very early the importance of applying quantum mechanics to biological problems [29–35], including hydrogen bond [33] and cancer-related issues [34, 35]. This is the subject of this investigation, where we consider hydrogen bonds between water and  $\text{MB}^+$  and calculate its structure and binding and the consequent changes in the spectroscopic properties of  $\text{MB}^+$ , a known dye in the photodynamic therapy of cancer. There

are several positions for binding of a water molecule in  $\text{MB}^+$ . The hydrogen bond on the top of the  $\text{MB}^+$  ring is excluded in this present study due to consideration of hydrophobic forces [22–24] and the formation of dimers  $\text{MB}^+:\text{MB}^+$ , known to occur depending on the concentration. Here we make an attempt to understand quantitatively the role played by hydrogen bond interactions. Thus we study three different cases where  $\text{MB}^+$  acts both as proton acceptor and proton donor. These cases are (i) the nitrogen atom of the central ring is the proton acceptor, (ii) the water is the proton acceptor with a binding at the hydrogen atom of the lateral ring; and (iii) the water is proton acceptor out of the central ring. In these cases multiple hydrogen bonds can be formed (see Fig. 1). Case (i) implies a conventional hydrogen bond. Hydrogen bonds similar to cases (ii) and (iii) have been recently analyzed and shown to be important in amino acids residues [36]. However, as we shall see in cases (ii) and (iii), the net positive charge on the sulfur atom of  $\text{MB}^+$  and the dipolar interaction influences on the binding and the position of the water molecule. We use a density-functional theory (DFT) [37] method to study these interactions between  $\text{MB}^+$  and water. We focus our attention on the geometry of the complex after the formation, the binding energy and the spectroscopic changes in the infrared (IR) and visible region. These results are aimed at understanding the influence of hydrogen bonds in the spectroscopic properties and photochemistry of  $\text{MB}^+$  in solution.

## Methodology

The use of DFT methods to study hydrogen bond interactions has increased in recent years [38–43]. Some successful results have been reported [38–41] but it has still not acquired full confidence [43]. It is generally believed that DFT approximates second-order Møller–Plesset perturbation theory [39, 40]. However, it has the advantage of including electron correlation effects with a computational effort that is only slightly higher than Hartree–Fock. Thus it has been suggested, from studies of hydrogen-bonded network of water [44], that DFT could be a valid alternative to Møller–Plesset perturbation theory. Because of the size of the systems considered here, DFT is a very attractive theoretical procedure. Full geometry optimizations are performed using analytical procedures in the density-functional Becke's three-parameter hybrid

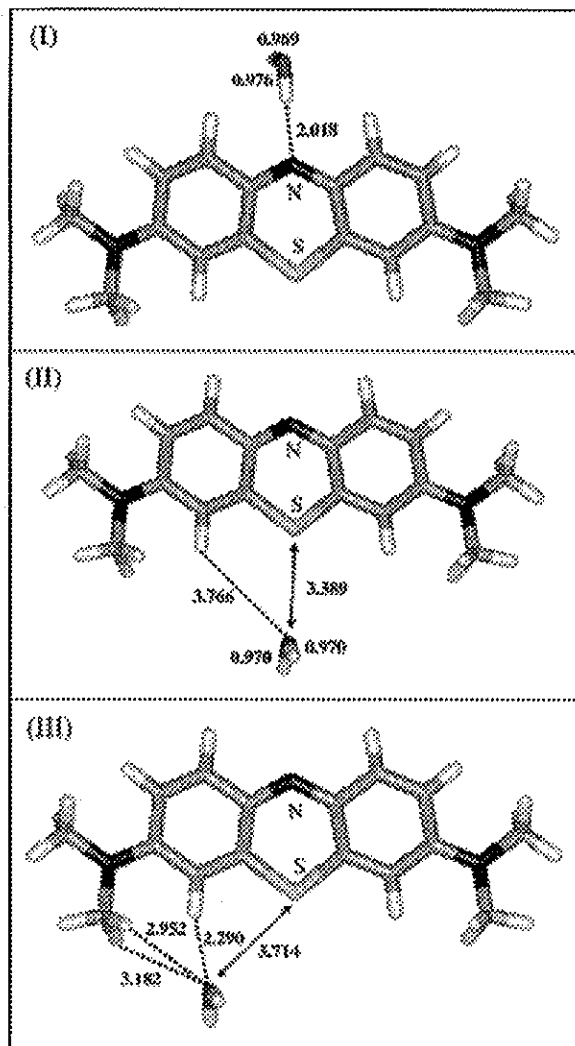


**FIGURE 1.** The calculated structure of the hydrogen bonded  $\text{MB}^+ \cdots \text{H}_2\text{O}$  systems. In case (II) and (III) the distance to the sulfur atom is also shown. All distances in angströms.

method using the Lee–Yang–Parr correlation functional, B3LYP [45, 46], with a 6-31+G(d) basis set. This is termed “B3LYP/6-31+G(d).” There is a total of 443 basis functions for the complex  $\text{MB}^+ \cdots \text{H}_2\text{O}$ , thus making the geometry optimization a considerable computational effort. Fully optimized structures are obtained for isolated water and  $\text{MB}^+$  and all the hydrogen bonded complexes  $\text{MB}^+ \cdots \text{H}_2\text{O}$  considered here. After obtaining these structures we analyze the geometric changes. Next we calculate the hessian (second derivatives) so as to obtain the

theoretical infrared spectrum.  $\text{MB}^+$  has a total of 108 vibrational modes. The complex  $\text{MB}^+ \cdots \text{H}_2\text{O}$  has in turn a total of 117 vibrational modes, where 6 are intermolecular vibrations not present in water or MB separately. This makes it clear that a comparison between the individual frequencies is difficult. There are several vibrational transitions below the  $400 \text{ cm}^{-1}$  spectrometer limit. These include not only the intermolecular vibrations but also a total of 21 vibrational modes of  $\text{MB}^+$ . These are the soft largely anharmonic modes not seen in the usual IR experiments. Because the vibrational shifts due to the complex formation are not expected to be large, we only analyze individually the most intense transitions. Finally, a comparison between the calculated total energies allows one to obtain the binding energy. These binding energies are then corrected to take into account the basis-set superposition error (BSSE) and the changes in zero-point vibrational energies (ZPE). All ab initio calculations have been performed with the program Gaussian98 [47].

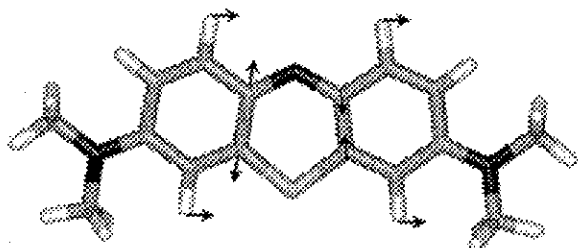
## Results

Figure 1 shows the structure and the relevant geometrical parameters of the three hydrogen-bonded  $\text{MB}^+ \cdots \text{H}_2\text{O}$  complexes. In isomer I, the water plays the role of proton donor and makes a hydrogen bond with the nitrogen atom of  $\text{MB}^+$ . As is usual, the OH distance not involved in the bond is unaffected but the other OH distance is lengthened compared to isolated water (from 0.969 Å to 0.976 Å). The NC distance of the central ring is also slightly increased but by a considerably smaller amount (from 1.336 Å to 1.337 Å). The hydrogen bond distance  $\text{HOH} \cdots \text{N}$  is calculated as 2.018 Å. In isomer II (Fig. 1) the distance between the oxygen atom of water and the sulfur atom of  $\text{MB}^+$  is calculated as 3.39 Å. As can be seen in Figure 1, the dipole moments of water and  $\text{MB}^+$  are aligned, suggesting a strong dipole interaction. A possible weak hydrogen bond with the lateral hydrogen atom, with a long distance of 3.77 Å, is obtained with water playing the role of a proton acceptor. The OH distances of water are found to be unaffected in this case but the HOH angle is slightly decreased from 105.5 to 104.9°. The possibility that this structure becomes a transition state with the use of other theoretical models cannot be discarded. Finally, we consider isomer III (Fig. 1). As we shall see this is the most bound of the three cases. The water molecule makes again multiple hydrogen bonds. We find a total of

three hydrogen bonds, as illustrated in Figure 1. These hydrogen bonds are formed between the oxygen atom of water and three hydrogen atoms of MB<sup>+</sup>. Two of these are more conventional hydrogen bonds with distances of 2.290 and 2.952 Å. The other is more loose involving a longer distance of 3.182 Å. The position of the water molecule in this isomer is influenced by the positive charge on the sulfur atom and the dipole interaction. For comparison, we also give the distance between the oxygen atom of water and the sulfur atom of MB<sup>+</sup>. Interestingly, we find only a negligible deformation of the water molecule that essentially preserves its bond distances and bond angle.

As MB<sup>+</sup> has 38 atoms there are 108 vibrational modes and an individual assignment of the corresponding modes is difficult and largely unnecessary. The experimental infrared spectrum of methylene blue shows eight intense characteristic vibrational transitions [48]. Experimentally, the most intense transitions are those obtained in the region 1200–1600 cm<sup>-1</sup>. The two transitions seen in the IR spectrum at 1142 cm<sup>-1</sup> and 1251 cm<sup>-1</sup> are calculated at, respectively, 1127 cm<sup>-1</sup> and 1319 cm<sup>-1</sup> and are those that suffer the largest shift (~10 cm<sup>-1</sup> to the high energy side) upon formation of the complex MB<sup>+</sup>··H<sub>2</sub>O. Both correspond, in approximate C<sub>2v</sub> notation, to b<sub>2</sub> vibrational modes of the isolated MB<sup>+</sup>. The first mode calculated at 1127 cm<sup>-1</sup> in MB<sup>+</sup> correspond to an in-plane asymmetric scissor mode, whereas that calculated at 1319 cm<sup>-1</sup> corresponds to an asymmetric in-plane twist of the C—C bond of the central ring with some H symmetric wag (Fig. 2), leading also to changes in the C=N and C—S stretches. This is calculated to shift by 10 cm<sup>-1</sup> in the case of the isomers I and II.

Now we consider the binding energy of the complex systems. Before showing the calculated binding energy, two aspects should be considered. First,



**FIGURE 2.** Illustration of the vibrational mode of MB<sup>+</sup> that is calculated to suffer the largest shift upon complexation with a hydrogen-bonded water. See text.

there is the basis-set superposition error (BSSE) that becomes operative for incomplete basis sets. This is corrected here by the counterpoise method [49] where the energy of the separate parts is calculated using the entire basis set of the complex. Second, the correction due to the difference in zero-point vibrational energy should also be considered. The intermolecular vibrational modes are largely anharmonic and as we discussed before, there are several intramolecular modes of MB<sup>+</sup> that are soft modes and anharmonic. Thus the use of the harmonic approximation gives only an estimate of the zero-point energy correction. The binding energies of the complex MB<sup>+</sup>··H<sub>2</sub>O using different DFT methods are shown in Table I, after correcting for BSSE. The difference in total energies for the separate parts and for the complex using B3LYP/6-31+G(d) gives a binding energy for isomer I of 4.0 kcal/mol. Taking into account the counterpoise correction to BSSE this value is decreased to 3.1 kcal/mol (Table I). If the difference due to zero-point energy correction is also included, this value is decreased further to 1.3 kcal/mol. This is only 0.7 kcal/mol higher than the *kT* energy at room temperature (0.6 kcal/mol), a very small binding. It may appear to be convenient to analyze this result with other density-functionals. Using the exchange correlation of Perdue [50], the so-called B3P86, and the Perdue–Wang 1991 gradient corrected functional [51], B3PW91, we obtain slightly different values of 3.5 kcal/mol and 2.5 kcal/mol, respectively. To clarify the role of the electron correlation contribution a Hartree–Fock calculation with the same basis set and the same geometry obtained with B3LYP/6-31+G(d) was made. The resulting binding energy is only 0.4 kcal/mol. This value is smaller than *kT* at room temperature and decreases further by including zero-point energy correction; i.e., at the HF level the system I is unbound. If the results shown in Table I are subtracted from the zero-point energy correction

**TABLE I**  
Calculated binding energy (kcal/mol) of MB<sup>+</sup>··H<sub>2</sub>O.<sup>a</sup>

Method	Isomer I	Isomer II	Isomer III
B3LYP/6-31+G(d)	3.1	3.3	5.1
B3P86/6-31+G(d)	3.5	3.3	5.2
B3PW91/6-31+G(d)	2.5	3.0	4.5
HF/6-31+G(d)	0.4	3.3	5.1

<sup>a</sup> Results shown include counterpoise correction to BSSE. See text and Figure 1.

obtained at the B3LYP/6-31+G(d) level, the highest binding energy is 1.7 kcal/mol (B3P86). Similar results are obtained for isomer II, except that all methods, including Hartree-Fock give a bound system. In this case the dipole interaction seems to be the stronger electrostatic contribution but we made no attempt to separate the different terms. As it can be seen isomer III is more bound than the previous two. At the B3LYP/6-31+G(d) it is bound by 5.1 kcal/mol. Similar results are obtained using the other two functionals. The difference between Hartree-Fock and B3LYP could be used as a quick measure of the electron correlation contribution to isomer III and this amounts to a negligible value. These isomer form multiple hydrogen bonds. An interesting aspect is the influence of these hydrogen bonds in the absorption spectrum.

MB<sup>+</sup> is one of the dyes used as a trigger in the activity of photodynamic therapy [12–16, 52–54]. In this, a possible mechanism is that MB<sup>+</sup> absorbs radiation in the first singlet state and after two intersystem crossings it transfers energy to O<sub>2</sub> in the excited singlet <sup>1</sup>Δ<sub>g</sub> state, with the photochemistry path: MB<sup>+</sup> + hν → (MB<sup>+</sup>)<sup>\*</sup> <sup>1</sup>π-π\* → (MB<sup>+</sup>)<sup>\*</sup> <sup>3</sup>π-π\* → O<sub>2</sub> (<sup>1</sup>Δ<sub>g</sub>). The singlet oxygen is a long lived and very reactive species that interacts with cytochrome-c leading to apoptosis [55, 56]. The solvent influence on the intramolecular transitions of O<sub>2</sub> has been analyzed before [57–59]. The photochemistry of MB<sup>+</sup> in interaction with biomolecules and membranes [60] indicates that other mechanisms of producing oxygen in singlet states are possible but both the singlet and triplet excited states are involved. Recent studies [61] have looked at the Soret band of Fe<sup>3+</sup> in cytochrome-c after photodynamical generation of O<sub>2</sub> (<sup>1</sup>Δ<sub>g</sub>). The effectiveness of

the energy transfer is dependent on the relative location of the first singlet and triplet excited states. MB<sup>+</sup> presents a well-known strong absorption at 664 nm (~15,000 cm<sup>-1</sup>) that gives its blue color. The change of these transitions in water is very important. To obtain the separate influence of the hydrogen bonds on the visible spectrum we have calculated the absorption transitions for isolated MB<sup>+</sup> and compared the result with that obtained for the corresponding MB<sup>+</sup> ··· H<sub>2</sub>O cluster. Thus using this super-molecular approach it is also possible to separate the contribution of the geometry distortion of MB<sup>+</sup> due to its interaction with water. Thus the structural contribution shown in Table II corresponds to the difference in the absorption transition of MB<sup>+</sup> using the optimized geometries of the isolated molecule and that obtained with the hydrogen-bonded water after removing the water molecule. The electronic contribution is then obtained after replacing the water molecule to its optimized position in the corresponding cluster. For all these calculations we have used the INDO/CIS [62] method as implemented in ZINDO [63]. In the case of isomers II and III we find a slight total blue shift of 80 cm<sup>-1</sup> and 57 cm<sup>-1</sup>, respectively. In the case of the isomer I we calculate a red shift of 15 cm<sup>-1</sup>. The separate contribution of the geometry distortion for isomers II and III gives a red shift that is compensated by the electronic blue shift. The influence of the hydrogen bonds on the lowest triplet state of MB<sup>+</sup> is also very mild. The largest shift is calculated for the least bound system (isomer I) that gives a red shift of ~200 cm<sup>-1</sup>. The influence of the hydrogen bonds on the solvation effects has also been calculated by the self-consistent reaction field (SCRFF), as implemented in ZINDO. Thus the solvatochromic

**TABLE II**  
Calculated shift (in cm<sup>-1</sup>) of the first singlet and triplet electronic transition of MB<sup>+</sup> due to the hydrogen bonds of the three isomers considered here (Fig. 1).<sup>a</sup>

	State	Structural	Electronic	Total HB	SCRFF
Isomer I	<sup>1</sup> π-π*	8	-23	-15	-59
	<sup>3</sup> π-π*	12	-205	-193	—
Isomer II	<sup>1</sup> π-π*	-23	113	80	60
	<sup>3</sup> π-π*	-4	50	46	—
Isomer III	<sup>1</sup> π-π*	-11	68	57	42
	<sup>3</sup> π-π*	0	0	0	—

<sup>a</sup> Structural contribution corresponds to the shift obtained by the rearrangement of the geometry of MB<sup>+</sup> alone. SCRFF includes the total solvation shift obtained by including the corresponding isomer in the cavity.

shifts obtained enclosing the  $\text{MB}^+ \cdots \text{H}_2\text{O}$  clusters in the cavity are also shown in Table II. The calculated SCRF solvent shift for the isolated  $\text{MB}^+$  in water is  $-15 \text{ cm}^{-1}$ , giving a very small red shift, as expected for  $\pi-\pi^*$  transitions. The amount of all these calculated shifts is in accord with the expected low influence of water on the photochemistry and spectroscopic properties of  $\text{MB}^+$ .

### Summary and Conclusions

Ab initio density-functional theory methods have been applied to study the  $\text{MB}^+ \cdots \text{H}_2\text{O}$  systems and the influence of complexation on the spectroscopic properties of  $\text{MB}^+$ . Using the B3LYP/6-31+G(d) method we have optimized the geometry of three isomers and compared with the separate moieties. A calculation of the changes in the infrared spectrum due to the complexation in the central ring shows that most of the intense transitions are unchanged. The largest change obtained was  $10 \text{ cm}^{-1}$  for the vibrational modes observed experimentally at  $1142 \text{ cm}^{-1}$  and  $1251 \text{ cm}^{-1}$ .

The binding energy is obtained after correcting the theoretical results for basis-set superposition error. The error due to zero-point harmonic vibrations is also approximately considered. The final calculated binding energy with B3LYP/6-31+G(d) is 3.1 kcal/mol, 3.3 kcal/mol and 5.1 kcal/mol for the three isomers I, II, and III, respectively. Using other functionals with the same basis set we find similar results to the B3LYP case, but B3PW91 gives the smaller binding. All considered, we conclude that the most bound system makes multiple hydrogen bonds and the water plays the role of proton acceptor. When these structures are used in the theoretical absorption spectrum we find only a minor change in the electronic spectroscopic properties of  $\text{MB}^+$  in solution. This relative stability is desired for the activity of  $\text{MB}^+$  as a trigger for photodynamic therapy.

### ACKNOWLEDGMENTS

It is our great privilege to dedicate this paper to a pioneer and great scientist Prof. Per-Olov Löwdin. For many years he has been of great support with several participations in summer schools, winter institutes and Sanibel Symposia. One of us (SC), in particular, would like to express gratitude for a generous 25 years of guidance and friendship. This work has been partially supported by CNPq and FAPESP (Brazil).

### References

1. Fowler, G. J. S.; Rees, R. C.; Devonshire, R. *Photochem Photobiol* 1990, 52, 489.
2. Aznar, J. A.; Bonamad, S.; Montoro, J. M.; Hurtado, C.; Cid, A. R.; Soler, M. A.; De Miguel, A. *Vox Sanguini* 2000, 79, 156.
3. Gabelova, A.; Pleskova, M. *Neoplasma* 2000, 47, 354.
4. Xiang, H. Y.; Chen, X. M.; Li, S. Q.; Xia, S.; Liu, A. X. *Chin J Anal Chem* 2000, 28, 1398; Li, W. Y.; Xu, J. G.; He, X. W. *Anal Lett* 2000, 33, 2453.
5. Teixeira, C. E.; Teixeira, S. A.; Antunes, E.; Nucci, G. *Toxicol* 2001, 39, 633.
6. Otaki, M.; Hirata, T.; Okagaki, S. *Wat Sci Tech* 2000, 42, 103.
7. Owada, T.; Yamada, Y.; Abe, H.; Hirayama, J.; Ikeda, H.; Sekiguchi, S.; Ikebuchi, K. *J Med Virol* 2000, 62, 421.
8. Fallon, M. B. *Ann Int Med* 2000, 133, 738; Vontanthen, R.; Beer, J. H.; Lauerburg, B. H. *Alcohol and Alcoholism* 2000, 35, 424.
9. Schenck, P.; Madl, C.; Rezaie-Majd, S.; Leht, S.; Muller, C. *Ann Int Med* 2000, 133, 701.
10. Gul, A.; Kotan, C.; Dilek, I.; Gul, T.; Tas, A.; Berktaş, M. *J Rep Fertil* 2000, 120, 225.
11. Mutzbauer, T. S.; Mueller, P. H. J.; Sigg, O.; Tetzlaff, K.; Neuerbauer, B. *Milit Med* 2000, 165, 849.
12. Dougherty, T. J. *Photochem Photobiol* 1987, 45, 879.
13. Kessel, D., Ed. *Methods in Porphyrin Photosensitization*; Plenum Press, New York, 1985.
14. Orth, K.; Beck, G.; Genze, F.; Ruck, A. *J Photochem Photobiol B-Biol* 2000, 57, 186.
15. Henderson, B. W.; Dougherty, T. J. *Photochem Photobiol* 1992, 55, 145.
16. Oscher, M. *J Photobiol B* 1997, 39, 1.
17. Dube, A.; Bansal, H.; Gupta, P. K. *Indian J Biochem Biophys* 2000, 37, 245.
18. Avila, V.; Bertolotti, S. G.; Criado, S.; Pappano, N.; Debatista, N.; Garcia, N. A. *Int J Food Sci Tech* 2001, 36, 25.
19. Fowler, G. J.; Rees, R. C.; Devonshire, R. *Photochem Photobiol* 1990, 52, 489.
20. Foote, C. S. *Science* 1968, 162, 963.
21. Wainwright, M. *Int J Antimicrob Ag* 2000, 16, 381.
22. Zhao, Z.; Malinowski, E. R. *App Spectr* 1999, 53, 1567.
23. Antonov, L.; Gergov, G.; Petrov, V.; Kubista, M.; Nygren, J. *Talanta* 1999, 49, 99.
24. Patil, K.; Pawar, R.; Talap, P. *Phys Chem Chem Phys* 2000, 2, 4313.
25. Gilli, G.; Gilli, P. *J Mol Struct* 2000, 552, 1.
26. Scheiner, S. *Hydrogen Bonding: A Theoretical Perspective*; Oxford Univ. Press, 1997; Stone, A. J. *The Theory of Intermolecular Forces*; Clarendon Press: Oxford, 1996.
27. Mukherjee, P.; Ghosh, A. K. *J Am Chem Soc* 1970, 92, 6419.
28. Löwdin, P.-O. *Int J Quantum Chem* 1995, 55, 77.
29. Löwdin, P.-O. *Rev Mod Phys* 1963, 35, 724.
30. Löwdin, P.-O. *Mutation Res* 1965, 2, 218.
31. Löwdin, P.-O. *Adv Quantum Chem* 1966, 2, 213.
32. Löwdin, P.-O.; MacIntyre, W. M. *Int J Quantum Chem Symp* 1968, 2, 207.

33. Löwdin, P.-O. *Ann NY Acad Sci* 1969, 158, 86.
34. Löwdin, P.-O. *Svenk Läkartidning* 1977, 74, 3419.
35. Löwdin, P.-O. *Int J Quantum Chem Symp QB* 1977, 4, 185.
36. Scheiner, S.; Kar, T.; Gu, Y. *J Biol Chem* 2001, 276, 9832.
37. Kohn, W. *Rev Mod Phys* 1999, 71, 1253.
38. Luque, F. J.; López, J. M.; Paz, M. L.; Vicent, C.; Orozco, M. *J Phys Chem A* 1998, 102, 6690.
39. Novoa, J. J.; Sosa, C. *J Phys Chem* 1995, 99, 15837.
40. Chandra, A. K.; Nguyen, M. T. *Chem Phys* 1998, 232, 299.
41. Siebrand, W.; Zgierski, M. Z. *Chem Phys Lett* 2001, 334, 127.
42. Rivelino, R.; Canuto, S. *Chem Phys Lett* 2000, 322, 207.
43. Del Bene, J. E.; Person, W. B.; Szczepaniak, K. *J Phys Chem* 1995, 99, 10705.
44. Suhai, S. *J Phys Chem* 1995, 99, 1172.
45. Becke, A. D. *Phys Rev A* 1988, 38, 3098; Becke, A. D. *J Chem Phys* 1993, 98, 5648.
46. Lee, C.; Yang, W.; Parr, R. G. *Phys Rev B* 1988, 37, 785.
47. Frisch, M. J.; Trucks, G. W.; Schlegel, H. B.; Scuseria, G. E.; Robb, M. A.; Cheeseman, J. R.; Zakrzewski, V. G.; Montgomery, Jr., J. A.; Stratmann, R. E.; Burant, J. C.; Dapprich, S.; Millam, J. M.; Daniels, A. D.; Kudin, K. N.; Strain, M. C.; Farkas, O.; Tomasi, J.; Barone, V.; Cossi, M.; Cammi, R.; Mennucci, B.; Pomelli, C.; Adamo, C.; Clifford, S.; Ochterski, J.; Petersson, G. A.; Ayala, P. Y.; Cui, Q.; Morokuma, K.; Malick, D. K.; Rabuck, A. D.; Raghavachari, K.; Foresman, J. B.; Cioslowski, J.; Ortiz, J. V.; Baboul, A. G.; Stefanov, B. B.; Liu, G.; Liashenko, A.; Piskorz, P.; Komaromi, I.; Gomperts, R.; Martin, R. L.; Fox, D. J.; Keith, T.; Al-Laham, M. A.; Peng, C. Y.; Nanayakkara, A.; Gonzalez, C.; Challacombe, M.; Gill, P. M. W.; Johnson, B.; Chen, W.; Wong, M. W.; Andres, J. L.; Gonzalez, C.; Head-Gordon, M.; Replogle, E. S.; Pople, J. A. *Gaussian 98, Revision A.7*; Gaussian, Inc.: Pittsburgh, PA, 1998.
48. *The Sadtler Standard Spectra*; Sadtler Research Laboratory: Philadelphia, 1970.
49. Boys, S. F.; Bernardi, F. *Mol Phys* 1970, 19, 5.
50. Perdew, J. P. *Phys Rev B* 1986, 33, 8822.
51. Burke, K.; Perdew, J. P.; Wang, Y. In *Electronic Density Functional Theory: Recent Progress and New Directions*; Dobson, J. F.; Vignale, G.; Das, M. P., Eds.; Plenum Press: New York, 1998.
52. Dougherty, T. J. *Semin Surg Oncol* 1986, 2, 24.
53. Kessel, D. *Oncol Res* 1992, 4, 219.
54. Saitow, F.; Nagaoka, Y. *Photochem Photobiol* 1997, 65, 902.
55. Yang, J.; Liu, X.; Bhalla, K.; Kim, C. N.; Ibrado, A. M.; Cai, J.; Peng, T.-I.; Jones, D. P.; Wang, X. *Science* 1997, 275, 1129.
56. Kluck, R. M.; Bossy-Wetzel, E.; Green, D. R.; Newmeyer, D. D. *Science* 1997, 275, 1132.
57. Minaev, B. F.; Lunell, S.; Kobzev, G. I. *J Mol Struct (Theorchem)* 1993, 284, 1.
58. Minaev, B. F. *J Applied Spectrosc* 1985, 42, 518.
59. Weldon, D.; Ogilby, P. R. *J Am Chem Soc* 1998, 120, 12978.
60. Junqueira, H. C.; Severino, D.; Gugliotti, M.; Baptista, M. S.; Baptista, M. S.; Indig, G. L. *J Phys Chem B* 1998, 102, 4678.
61. Nantes, I. L.; Faljoni-Alário, A.; Vercesi, A. E.; Santos, K. E.; Bechara, E. J. H. *Free Radic Biol Med* 1998, 25, 546; Nantes, I. L. private communication.
62. Ridley, J.; Zerner, M. C. *Theoret Chim Acta* 1973, 32, 111.
63. Zerner, M. C. *ZINDO: A semi-empirical program package*, University of Florida, Gainesville, FL 32611.